UDC 666.943.3

H.N. Shabanova [a], S.M. Logvinkov [b], V.N. Shumeyko [a], A.N. Korohodska [a], V.A. Sviderskii [c], G.V. Lisachuk [a], M.D. Sakhnenko [a], V.V. Voloshchuk [a], D.A. Kudii [a]

OPTIMIZATION OF THE RATIO OF ADJACENT AGGREGATE FRACTIONS FOR SLAG-ALKALI BINDER CONCRETE

[a] National Technical University «Kharkiv Polytechnic Institute», Kharkiv, Ukraine
[b] O.M. Beketov National University of Urban Economy in Kharkiv, Kharkiv, Ukraine
[c] National Technical University of Ukraine «Igor Sikorsky Kyiv Polytechnic Institute», Kyiv, Ukraine

The results of determining the rational content of granite gravel and sand fractions for concrete products subjected to vibration pressing, aimed at achieving a high degree of compaction, are presented. The analysis of experimental data consecutively narrowed the concentration range of mixture compositions with high values of bulk density and compaction coefficients, identifying the optimal composition of charge fractions (wt.%): 37.5 – 5–10 mm granite gravel; 25 – 2–5 mm granite gravel; and 37.5 – 0–0.3 mm sand. The simplex-lattice method was used for mathematical processing of the experimental results. Based on the analysis of regression equations and «composition vs. property» diagrams, the regularities of changes in bulk density under loading and the compaction coefficient of three-fraction mixtures, depending on their composition, were established. Deviations between experimental and calculated data were 1.5–2.8% and 2.1–3.2% for bulk density under loading and compaction factor, respectively, confirming a high degree of accuracy in predicting the specified properties of three-fraction mixtures and the relevance of the obtained mathematical models.

Keywords: workability, three-fraction mixture, granite gravel, sand, mathematical modeling, Scheffe's plans, regression equation.

DOI: 10.32434/0321-4095-2024-157-6-136-143

Introduction

Sustainable development has been defined by the United Nations as «development that meets the needs of the present without compromising the ability of future generations to meet their own needs – by attempting to balance social, economic and environmental effects». Among the key areas of sustainable development, the modern building materials industry resonates with Goal 9 «Build sustainable infrastructure, promote inclusive and sustainable industrialization and foster innovation»[1].

Achievements in sustainable construction and the green building movement in recent decades have encouraged materials scientists to study building materials and their production methods in detail. Modern concrete science plays an invaluable role in achieving the goals of reducing ecological harm to the environment and providing the most beneficial use of concrete in sustainable design, with a focus on the environmental impact as well as the health and safety of workers and consumers.

For practical use in green building, concrete

[1] Resolution adopted by the United Nations General Assembly on 6 July 2017 [without reference to a Main Committee (A/71/L.75)] 71/313. Work of the Statistical Commission pertaining to the 2030 Agenda for Sustainable Development. https://documents.un.org/doc/undoc/gen/n17/207/63/pdf/n1720763.pdf (date of application 01.08.2024).

should be strong, durable, and preferably immune to any environmental factors causing damage or deterioration. It must have the ability to withstand elevated or reduced ambient temperatures to insulate interior spaces, not to mention its ability to provide soundproofing, making it an ideal building material anywhere in the world. Efficiently used, quality engineered concrete can contribute greatly to the creation of sustainable buildings, bridges and other infrastructures necessary for the successful future of any country [1].

Concrete has been popular for many decades due to three distinctive characteristics: plasticity, durability and economy. In its mobile state, concrete can be poured into any shape, filling any space, covering any surface. After setting and hardening, it retains its shape, becoming stronger, harder and more stable over time [2,3].

Concrete can be waterproof, storm resistant and fire resistant if it is made according to the necessary requirements from quality raw materials. This provides concrete structures with long-term trouble-free operation.

Practicing civil engineering specialists favor concrete compositions based on classical or modern methods of concrete selection. The methods used are experimental (laboratory tests), empirical (semi-empirical) and analytical. Currently, the selection of concrete composition is focused on methods that are based on numerical modeling [4].

The basis of quality concrete is the proper selection of aggregate particle size distribution, which allows achieving the most dense packing of grains and, as a consequence, increased compressive strength, water and frost resistance [2,3].

As the most common coarse aggregate, granite gravel of different fractions is used, and sands with different grain size modulus are used as a fine-grained component. The hydraulically active component of the developed mixes is slag-alkali binder [5]. In previous studies, when using gravel of different fractions in the concrete composition, the content of fine and medium fractions of aggregate was limited, which led to further deterioration of the quality of concrete products due to reduced workability [6].

In connection with the above-mentioned, the purpose of the work was to clarify the developed experimental methodology for selecting a rational granulometric composition of three-fractional charge containing granite gravel and sand, taking into account the increased workability for pressed and vibro-pressed products.

Materials and methods

Granite gravel (Poltava region, Shmatkivske field) of fractions 5−10 mm (designated as X), 2−5 mm (designated as Y), as well as sand (Kremenchuk city, PJSC «Kremenchuk River Port») with grain size less than 0.3 mm (designated as Z) were used for experimental studies. The components of the charge were dosed, mixed and poured into the measuring device, a cylindrical container with a plug and a load with a rod and ruler. A ball-shaped copter was suspended coaxially with respect to the cylindrical container. For the tests, the copter was moved away from the vertical axis at a distance of 400 mm (between the center of the ball and the center of intersection of the cylindrical vessel axis with the concrete base) and released, which resulted in a point impact of the ball against the outer part of the measuring device and shaking of the charge in it. After each 0, 5, 10 and 15 impacts, the height of the charge layer in the cylindrical vessel was measured. According to the measurement results, the corresponding bulk density of the charge under the load (ρ_i, where the number of copra beats i=0; 5; 10; 15) and the packing factor of particles in the corresponding charge as the ratio of the maximum value of the height of the charge layer to its minimum value (K_y) were calculated.

For convenience in analyzing the test results, the charge compositions were graphically represented by points, the coordinates of which are shown by the lower indices (k, l, m) in the formula entry $X_kY_lZ_m$, which corresponds to the content of the corresponding fraction (in mass per cent) in a particular charge.

The use of methods of experiment design allows reducing considerably the volume of experiment at studying multicomponent systems. In addition, there is no need in spatial representation of complex surfaces, as properties can be determined from equations. At the same time, the possibility of graphical interpretation of the results is preserved. To generalize the regularities of changes in ρ_i and K_y with changes in the composition of the charge under study, we used the method of mathematical planning of experiment - the Scheffe's simplex lattice method [4].

Results and discussion

Based on the results of previous studies, in order to clarify the ratio of the number of adjacent aggregate fractions in a multidimensional space, a region bounded by the elements of the structure of three contiguous triangles, which highlight the concentration region in the form of a trapeze, was selected (Fig. 1).

It is in this area that the experimental search for charges with possibly higher compactibility under similar test conditions was carried out. The data for calculations for the charges corresponding to the triangle vertices are given in Table 1.

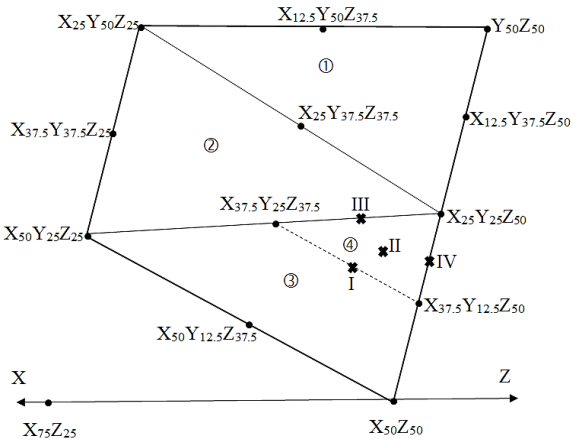

Fig. 1. Points and formula entry of the charge for tests in the selected area of the concentration triangle (explanation of the points of the compositions marked with crosses and numbered with Roman numerals is given later in the text)

For further tests, seven charges were selected, the compositions of which belong to the midpoints of the triangles sides that make up the trapezoidal concentration region in Fig. 1; the results of calculations of ρ_i and K_y values are summarized in Table 2.

For all tested charge compositions (Table 2), the regularities of changes in ρ_i and K_y are preserved: the charge compact as the number of copra beats increases. It is important to point out that composition No. 7 (Table 2) has a value of ρ_{15} higher than all other ones, including those previously studied (Table 1). Also high values of ρ_{15} are observed for charge compositions No. 4 and No. 3 (Table 2), but the value of ρ_{15} for the previously tested composition No. 5 (Table 1) is higher.

In accordance with the maximum values of ρ_{15} for compositions No. 7 (Table 2), No. 5 (Table 1) and No. 3 (Table 2), there are formal reasons for the subsequent search for rational charge compositions in the concentration region limited by the points of the above-mentioned compositions. However, there are arguments against it, because between the points of compositions No. 7 and No. 3 (Table 2), there is located (Fig. 1) the point of already investigated composition No. 6 (Table 2), for which the value of ρ_{15} is one of the lowest (Table 2). Therefore, in order to further narrow down the search area for rational compositions, it was decided to test those that are below the segment between the points of compositions No. 7 (Table 2) and No. 5 (Table 1), specifically, four compositions: three of them correspond to the midpoints of the sides of a regular triangle with vertices corresponding to the points of compositions No. 7 (Table 2), No. 5 (Table 1) and No. 5 (Table 2), and also one composition corresponding to the point of the center of symmetry of the marked triangle. These compositions are numbered with Roman numerals and marked with crosses in Fig. 1. The results of calculations of ρ_i and K_y for the compositions of charges I–IV are presented in Table 3.

Table 1

Results of calculations by triangle vertices according to the experimental design (Fig. 1)

No.	Formulaic entry of the composition	ρ_0	ρ_5	ρ_{10}	ρ_{15}	K_y
1	$X_{50}Z_{50}$	1.710	1.790	1.820	1.846	1.080
2	$Y_{50}Z_{50}$	1.676	1.757	1.807	1.833	1.094
3	$X_{25}Y_{50}Z_{25}$	1.613	1.654	1.687	1.710	1.060
4	$X_{50}Y_{25}Z_{25}$	1.710	1.757	1.807	1.820	1.064
5	$X_{25}Y_{25}Z_{50}$	1.794	1.833	1.873	1.887	1.052

Table 2

Results of calculations according to the experimental design (Fig. 2)

No.	Formulaic entry of the composition	ρ_0	ρ_5	ρ_{10}	ρ_{15}	K_y
1	$X_{50}Y_{12.5}Z_{37.5}$	1.710	1.769	1.807	1.820	1.064
2	$X_{37.5}Y_{37.5}Z_{25}$	1.699	1.757	1.794	1.807	1.064
3	$X_{12.5}Y_{50}Z_{37.5}$	1.665	1.820	1.846	1.873	1.125
4	$X_{12.5}Y_{37.5}Z_{50}$	1.733	1.794	1.833	1.860	1.073
5	$X_{37.5}Y_{12.5}Z_{50}$	1.676	1.794	1.820	1.833	1.094
6	$X_{25}Y_{37.5}Z_{37.5}$	1.676	1.757	1.794	1.820	1.086
7	$X_{37.5}Y_{25}Z_{37.5}$	1.873	1.887	1.916	1.930	1.030

Table 3

Results of ρ_i and K_y calculations for charge compositions I–IV

No.	Formulaic entry of the composition	ρ_0	ρ_5	ρ_{10}	ρ_{15}	K_y
I	$X_{37.5}Y_{18.75}Z_{43.75}$	1.644	1.733	1.782	1.807	1.099
II	$X_{33.33}Y_{20.83}Z_{45.84}$	1.757	1.820	1.860	1.874	1.066
III	$X_{31.25}Y_{25}Z_{43.75}$	1.800	1.782	1.807	1.883	1.072
IV	$X_{31.25}Y_{18.75}Z_{50}$	1.757	1.820	1.873	1.901	1.082

None of charges I–IV (Table 3) has a value of ρ_{15} greater than that of charge No. 7 (Table 2). In Table 3, the maximum value of ρ_{15} can be observed for charge No. IV and a slightly lower value for charge No. II. Exactly the points of charge No. 7 (Table 2) and charges No. II and IV (Table 3) make up a triangle, highlighting the most rational concentration area of granulometric composition. Moreover, the composition No. 7 (Table 2) should be recognized as optimal at this stage of research. For further experiments, we chose a promising concentration area in the above triangle: closer to the top of the sharp angle corresponding to the point of composition No. 7 (Table 2, and Fig. 1).

The availability of experimental results for the charge compositions corresponding to the vertices and midpoints of the sides of each of the three triangles within the trapezoidal concentration area (Tables 1 and 2) justified the application of the simplex-lattice Scheffe's method using a second-order polynomial for each triangle. The distribution of the ρ_{15} isolines within the concentration region, defined by the vertices of the first triangle (Fig. 2), shows a monotonic increase in ρ_{15} values. This increase extends from the charge composition point $X_{25}Y_{50}Z_{25}$ at the apex of the triangular lattice toward its central region, with two prominent directions of further increase: towards $X_{25}Y_{25}Z_{50}$ (where ρ_{15} values exceed 1.88) and along the side of the triangular lattice between $X_{25}Y_{50}Z_{25}$ and $Y_{50}Z_{50}$. The highest ρ_{15} values (greater than 1.89) are observed within the concentration range (wt.%): 63–93% $Y_{50}Z_{50}$, 7–37% $X_{25}Y_{50}Z_{25}$, and up to 7% $X_{25}Y_{25}Z_{50}$. Notably, this concentration range also exhibits high K_y values, as shown by comparing Figs. 2 and 3.

In Fig. 3, the region of compositions with high K_y values (greater than 1.1) is extensive and completely covers the region of compositions with high ρ_{15} values noted in Fig. 2.

The second triangle of the trapezoidal region (Fig. 1) is characterized by higher values of ρ_{15} and a monotonic growth in the direction from the composition point $X_{25}Y_{50}Z_{25}$, corresponding to the top of the triangular simplex lattice (Fig. 4), to the side $X_{25}Y_{25}Z_{50}$–$X_{50}Y_{25}Z_{25}$. On this side, the isoline ρ_{15}>1.93

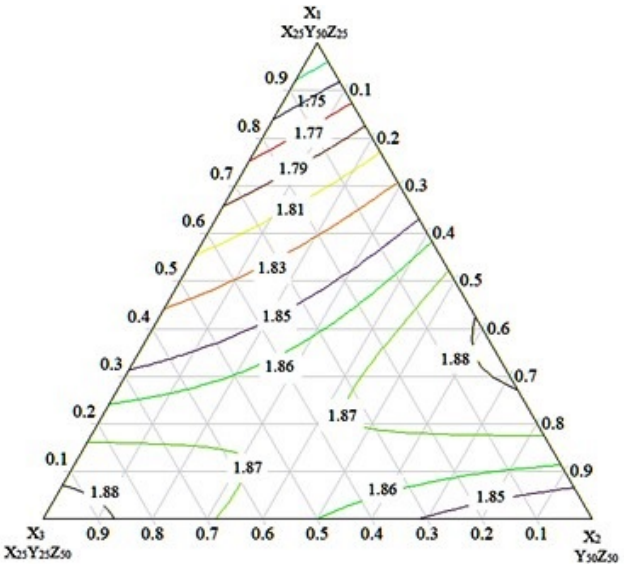

Fig. 2. Isolines of c_{15} values according to the regression equation $\rho_{15}=1.71x_1+1.833x_2+1.887x_3+0.406x_1x_2+0.086x_1x_3$ in the concentration limits of the first triangle of compositions

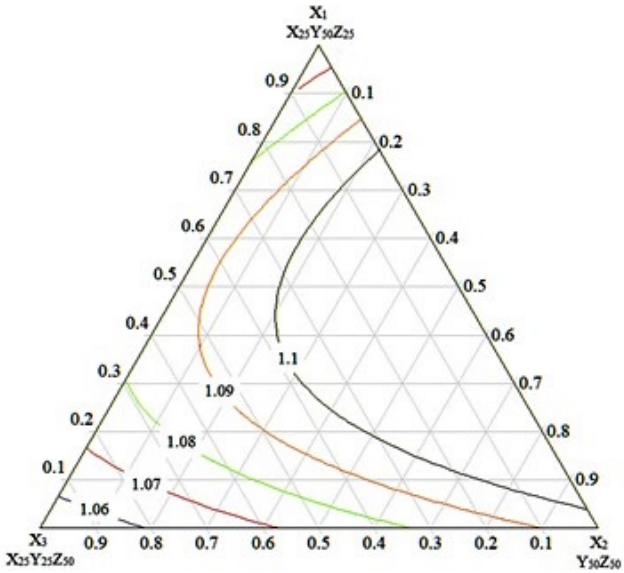

Fig. 3. Isolines of K_y values according to the regression equation $K_y=1.06x_1+1.094x_2+1.052x_3+0.192x_1x_2+0.12x_1x_3$ in the concentration limits of the first triangle of compositions

highlights a narrow concentration region ($X_{50}Y_{25}Z_{25}$ from 29 to 50 wt.%) with maximum values of ρ_{15}. At the same time, the marked region is not characterized by simultaneously high values of K_y, which is clearly evident from Fig. 5.

In the considered triangle of the simplex-lattice, the values of K_y are lower than in the first triangle (comparing Figs. 3 and 5). Isolines with maximal K_y values greater than 1.08 tend to the side $X_{25}Y_{25}Z_{50}$–$X_{25}Y_{50}Z_{25}$ at the content of the last composition from 30 to 75 wt.%.

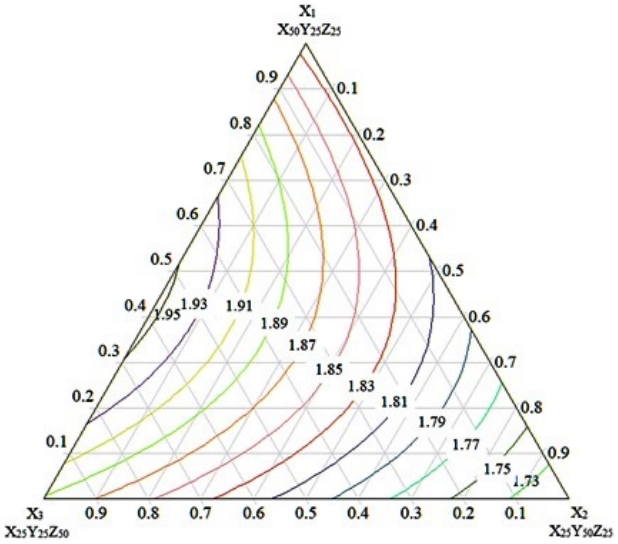

Fig. 4. Isolines of ρ_{15} values according to the regression equation $\rho_{15}=1.82x_1+1.71x_2+1.887x_3+0.168x_1x_2+0.306x_1x_3+0.086x_2x_3$ in the concentration limits of the second composition triangle

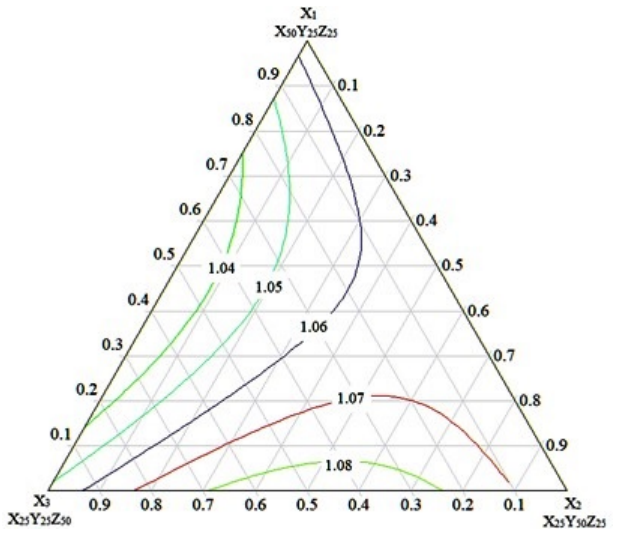

Fig. 5. Isolines of K_y values according to the regression equation $K_y=1.064x_1+1.06x_2+1.052x_3+0.008x_1x_2-0.112x_1x_3+0.12x_2x_3$ in the concentration limits of the second triangle of compositions

In the third triangle of the trapezoidal region (Fig. 1), the values of ρ_{15} are also, as in the second triangle, lower than in the first of them (comparing Figs. 2, 4 and 6). Isolines with ρ_{15}=1.86 highlight in the simplex lattice a wide band of charge compositions with values ρ_{15}=1.87–1.88.

At the same time, in the central zone of this band a saddle-shaped region with reduced values of ρ_{15} is noted, and in the direction to the top $X_{25}Y_{25}Z_{50}$ and side $X_{50}Z_{50}$–$X_{50}Y_{25}Z_{25}$ (content of the latter 57–72 wt. %), ρ_{15} increases up to the limiting value of 1.88 in this case.

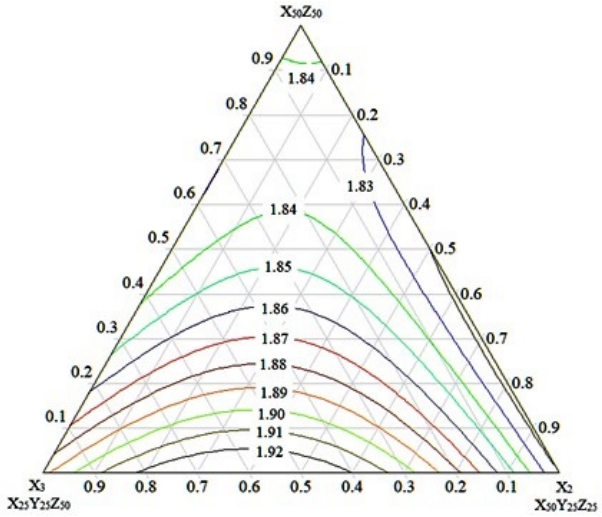

Fig. 6. Isolines of ρ_{15} values according to the regression equation $\rho_{15}=1.846x_1+1.82x_2+1.887x_3-0.052x_1x_2-0.134x_1x_3+0.306x_2x_3$ in the concentration limits of the third triangle of compositions

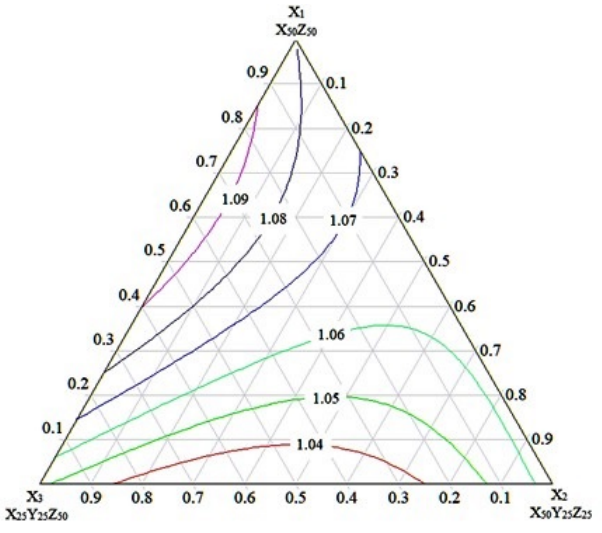

Fig. 7. Isolines of K_y values according to the regression equation $K_y=1.08x_1+1.064x_2+1.053x_3-0.032x_1x_2+0.112x_1x_3-0.112x_2x_3$ in the concentration limits of the third triangle of compositions

Comparison of Figs. 6 and 7 indicates that in the analyzed case the concentration region of compositions with high values of ρ_{15} is not simultaneously marked by high values of K_y.

Isoline K_y=1.09 highlights the optimal for this case relatively narrow zone of charge compositions within the content (wt.%): 30–61% $X_{50}Z_{50}$, 39–70% $X_{25}Y_{25}Z_{50}$ and 0–10% $X_{50}Y_{25}Z_{25}$.

Analyzing the totality of results of mathematical planning of experiments on all three triangles of the trapezoidal area (Fig. 1), it should be noted that the search for promising compositions was carried out in the right direction, because the isolines with high values of ρ_{15} pass between the points of charge compositions $X_{50}Y_{25}Z_{25}$ and $X_{25}Y_{25}Z_{50}$. The compositions with maximum values of ρ_{15} are concentrated on the corresponding sides of simplex-lattice triangles (Figs. 4 and 6), and according to Fig. 2, the isolines with high values of ρ_{15} are also drawn to the point of composition $X_{25}Y_{25}Z_{50}$.

At the same time, the expected values of K_y in the marked promising region of compositions will not be maximal: in the range of 1.04–1.06 based on Figs. 3, 5 and 7. It is possible to predict an additional area of promising compositions not covered by the experiments: a triangle with vertices $X_{25}Y_{25}Z_{50}$–$X_{37.5}Y_{25}Z_{37.5}$–$X_{25}Y_{37.5}Z_{37.5}$ (Fig. 1), within which isolines ρ_{15} have high values (Figs. 4 and 6).

For the last fourth series of experimental data (Table 3), the experimental design took into account the presence of results for ρ_{15} and K_y for the points of charge compositions at the vertices, at the midpoints of the sides and in the center of symmetry of the triangle $X_{25}Y_{25}Z_{50}$–$X_{37.5}Y_{12.5}Z_{50}$–$X_{37.5}Y_{25}Z_{37.5}$, which determined the search for the regression equation in the form of a polynomial of incomplete third order. The graphical representation of the values of ρ_i calculated for this case is presented in Fig. 8.

In Fig. 8, two concentration regions with high values of ρ_{15} (more than 1.90) are clearly delineated by isolines with ρ_{15}=1.88: a narrow zone near the side $X_{25}Y_{25}Z_{50}$–$X_{37.5}Y_{12.5}Z_{50}$ (within concentrations (wt.%): 15–51% $X_{37.5}Y_{12.5}Z_{50}$, 49–85% $X_{25}Y_{25}Z_{50}$ and 0–7% $X_{37.5}Y_{25}Z_{37.5}$) and an almost triangular in shape region near the apex of the triangle $X_{37.5}Y_{25}Z_{37.5}$.

The peaks of this region correspond to the following: (1) 92 wt.% of $X_{37.5}Y_{25}Z_{37.5}$ content on the side $X_{37.5}Y_{12.5}Z_{50}$–$X_{37.5}Y_{25}Z_{37.5}$; (2) 15 wt.% of $X_{25}Y_{25}Z_{50}$ content on the side $X_{25}Y_{25}Z_{50}$–$X_{37.5}Y_{25}Z_{37.5}$; and (3) the composition point of the top of the simplex-lattice triangle itself $X_{37.5}Y_{25}Z_{37.5}$. It is these areas of charge compositions should be singled out as promising for further experimental studies.

The values of K_y in the noted promising areas are low, which is in agreement with the previously analyzed results of mathematical planning K_y in the triangle of charge compositions $X_{50}Y_{25}Z_{25}$–$X_{25}Y_{25}Z_{50}$–$X_{37.5}Y_{12.5}Z_{50}$ (Fig. 1), which includes the triangle studied in this case (Fig. 9). The narrow zone of charge compositions with high values of K_y is highlighted in Fig. 9 by the isoline ρ_{15}=1.1, and the zone itself is located near the side of the triangle $X_{37.5}Y_{12.5}Z_{50}$–$X_{37.5}Y_{25}Z_{37.5}$, but from the opposite end, not where the maximum values of ρ_{15} are marked.

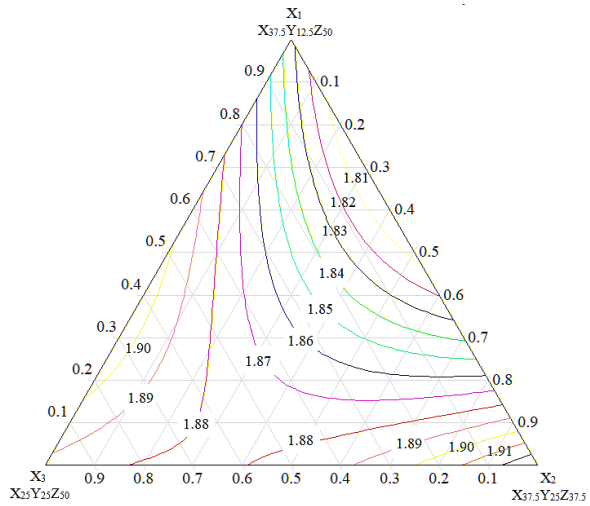

Fig. 8. Isolines of ρ_{15} values according to the regression equation $\rho_{15}=1.833x_1+1.93x_2+1.887x_3-0.298x_1x_2+0.164x_1x_3-0.102x_2x_3+0.078x_1x_2x_3$ in the concentration limits of the fourth triangle of compositions

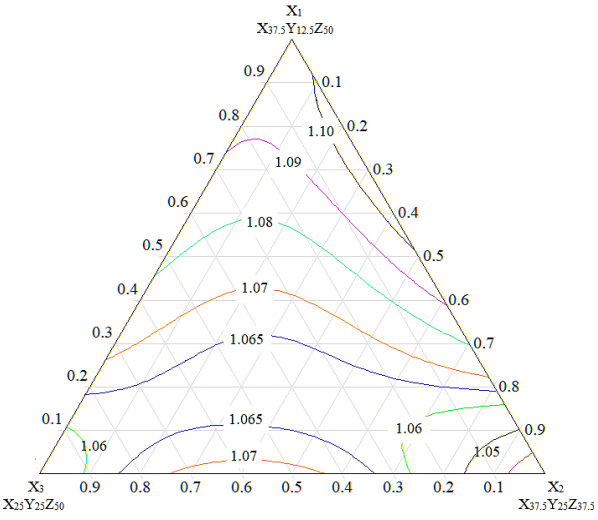

Fig. 9. Isolines of K_y values according to the regression equation $K_y=1.094x_1+1.03x_2+1.052x_3+0.148x_1x_2+0.036x_1x_3+0.124x_2x_3-0.726x_1x_2x_3$ in the concentration limits of the fourth triangle of compositions

To check the relevance of the obtained regression equations and the possibility of using their graphical interpretations in the prediction of charge compositions with predetermined values of ρ_{15} and K_y, a control experiment was performed for the reference charge composition $X_{31.25}Y_{21.875}Z_{46.875}$, which belongs to the concentration region of the triangle $X_{25}Y_{25}Z_{50}$–$X_{37.5}Y_{12.5}Z_{50}$–$X_{37.5}Y_{25}Z_{37.5}$. Checking the calculated values of ρ_{15} and K_y by regression equations in the refined concentration region of the simplex-lattice, in which the reference composition of the charge is directly located (Figs. 8 and 9), showed the following deviations from the experimental values: with an excess of 1.5% and a decrease of 2.1%, respectively. Such small deviations of calculated and experimental data limited further statistical analysis of the adequacy of the obtained regression equations, providing high accuracy of prediction of the sought characteristics, and therefore the mathematical models are relevant.

The predicted availability of the search in further experiments, closer to the conditions of vibrocompression, provides for the study of the charge between the compositions $X_{25}Y_{25}Z_{50}$ and $X_{37.5}Y_{25}Z_{37.5}$, which allows us to graphically interpret the relationship between the fractions of the charge and their content (Fig. 10).

Conclusions

The results of determination of rational content of fractions of granite gravel and sand for concrete ejected products, meeting the conditions of achievement of high degree of compactability are presented.

Analysis of the results of experimental studies successively narrowed the concentration area of charge compositions with high values of their bulk density and compaction coefficients, highlighting the rational composition of charge fractions (wt.%): 37.5% – fraction 5–10 mm granite gravel; 25% – fraction 2–5 mm granite gravel; and 37.5% – fraction 0–0.3 mm sand. For mathematical processing of experimental results, simplex-lattice method was used. According to the results of analysis of regression equations and diagrams «composition vs. property», the regularities of changes in bulk density under loading and compaction factor of three-fractional charges depending on their composition were established. The deviations between experimental and calculated data amounted to 1.5–2.8% and 2.1–3.2% for bulk density under loading and compaction factor, respectively, which confirmed a high degree of accuracy in predicting the specified properties of three-fraction charge and relevance of the obtained mathematical models. According to the results of mathematical processing of experimental data, the concentration area of charge with variation of compositions within the limits of changes in the content of fractions (wt.%) is predicted promising for practical application: 25–37.5% granite gravel 5–10 mm; 25% granite gravel 2–5 mm; and 25–50% sand 0–0.3 mm.

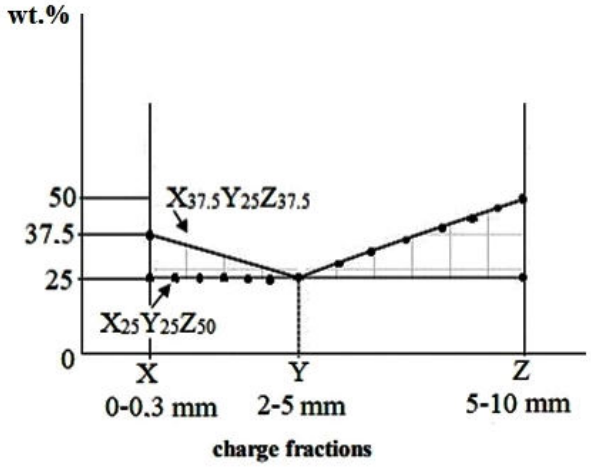

Fig. 10. Region of rational content of fractions in charge (with high values of ρ_{15})

Acknowledgments

The research was carried out with the grant support of the National Research Foundation of Ukraine within the framework of the project 2021.01/0316 «Development of composite materials for road construction based on multi-ton waste».

REFERENCES

1. *Sabnis M.G.* Green building with concrete. Sustainable design and construction. 2nd edition. – Boca Raton: CRC Press, 2015. – 459 p.

2. *Neville A.M., Brooks J.J.* Concrete technology textbook. 2nd edition. – Pearson, 2010. – 460 p.

3. *Obla K.H.* Improving concrete quality. – Boca Raton: CRC Press, 2014. – 214 p.

4. *Kumar S., Barai S.V.* Concrete fracture models and applications. – Berlin: Springer-Verlag, 2011. – 262 p.

5. *Development* of compositions of slag-alkaline binding materials for pavement products / Shabanova G.M., Korogodska A.M., Shumeiko V.M., Borysenko O.M., Lisachuk G.V., Kryvobok R.V., et al. // Voprosy Khimii i Khimicheskoi Tekhnologii. – 2023. – No. 5. – P.147-154.

6. *The effect* of hardening activators on the physical and mechanical properties of slag-alkaline binding materials / Shabanova G.M., Korogodska A.M., Shumeiko V.M., Shchukina L.P., Lisachuk G.V., Kryvobok R.V., et al. // Voprosy Khimii i Khimicheskoi Tekhnologii. – 2023. – No. 5. – P.155-162.

Received 19.08.2024

ОПТИМІЗАЦІЯ СПІВВІДНОШЕННЯ СУМІЖНИХ ФРАКЦІЙ ЗАПОВНЮВАЧА ДЛЯ БЕТОНУ НА ШЛАКОЛУЖНОМУ В'ЯЖУЧОМУ

Г.М. Шабанова, С.М. Логвінков, В.М. Шумейко, А.М. Корогодська, В.А. Свідерський, Г.В. Лісачук, М.Д. Сахненко, В.В. Волощук, Д.А. Кудій

Наведено результати визначення раціонального вмісту фракцій гранітного гравію та піску для бетонних виробів, які вібропресуються, з метою досягнення високого ступеня ущільнюваності. Аналіз результатів експериментальних досліджень дозволив послідовно звузити концентраційну ділянку складів шихт, що мають високі значення насипної щільності та коефіцієнтів ущільнення, визначивши раціональний склад фракцій шихти (мас.%): 37,5 – фракція 5–10 мм гранітного гравію, 25 – фракція 2–5 мм гранітного гравію та 37,5 – фракція 0–0,3 мм пісок. Для математичного оброблення результатів експериментів застосовано симплекс-решітчастий метод моделювання. За результатами аналізу рівнянь регресії та побудови діаграм «склад–властивість» встановлено закономірності змін насипної щільності під привантаженням і коефіцієнта ущільнення трифракційних шихт залежно від їх складу. Відхилення між експериментальними та розрахунковими даними склали 1,5–2,8% за насипною щільністю під привантаженням та 2,1–3,2% за коефіцієнтом ущільнення, що підтвердило високу точність прогнозування заданих властивостей трифракційних шихт і релевантність отриманих математичних моделей.

Ключові слова: зручноукладальність, трифракційна шихта, гранітний гравій, пісок, математичне моделювання, плани Шеффе, рівняння регресії.

OPTIMIZATION OF THE RATIO OF ADJACENT AGGREGATE FRACTIONS FOR SLAG-ALKALI BINDER CONCRETE

H.N. Shabanova [a], S.M. Logvinkov [b], V.N. Shumeyko [a], A.N. Korohodska [a, *], V.A. Sviderskii [c], G.V. Lisachuk [a], M.D. Sakhnenko [a], V.V. Voloshchuk [a], D.A. Kudii [a]

[a] **National Technical University «Kharkiv Polytechnic Institute», Kharkiv, Ukraine**

[b] **O.M. Beketov National University of Urban Economy in Kharkiv, Kharkiv, Ukraine**

[c] **National Technical University of Ukraine «Igor Sikorsky Kyiv Polytechnic Institute», Kyiv, Ukraine**

[*] **e-mail: alla-korogodskaya@ukr.net**

The results of determining the rational content of granite gravel and sand fractions for concrete products subjected to vibration pressing, aimed at achieving a high degree of compaction, are presented. The analysis of experimental data consecutively narrowed the concentration range of mixture compositions with high values of bulk density and compaction coefficients, identifying the optimal composition of charge fractions (wt.%): 37.5 – 5–10 mm granite gravel; 25 – 2–5 mm granite gravel; and 37.5 – 0–0.3 mm sand. The simplex-lattice method was used for mathematical processing of the experimental results. Based on the analysis of regression equations and «composition vs. property» diagrams, the regularities of changes in bulk density under loading and the compaction coefficient of three-fraction mixtures, depending on their composition, were established. Deviations between experimental and calculated data were 1.5–2.8% and 2.1–3.2% for bulk density under loading and compaction factor, respectively, confirming a high degree of accuracy in predicting the specified properties of three-fraction mixtures and the relevance of the obtained mathematical models.

Keywords: workability; three-fraction mixture; granite gravel; sand, mathematical modeling; Scheffe's plans; regression equation.

REFERENCES

1. Sabnis MG. *Green building with concrete. Sustainable design and construction*. 2nd edition. Boca Raton: CRC Press; 2015. 459 p. doi: 10.1201/b18613.

2. Neville AM, Brooks JJ. *Concrete technology textbook*. 2nd edition. Pearson; 2010. 460 p.

3. Obla KH. *Improving concrete quality*. Boca Raton: CRC Press; 2014. 214 p. doi: 10.1201/b17098.

4. Kumar S, Barai SV. *Concrete fracture models and applications*. Berlin: Springer-Verlag; 2011. 262 p. doi: 10.1007/978-3-642-16764-5.

5. Shabanova GM, Korogodska AM, Shumeiko VM, Borysenko OM, Lisachuk GV, Kryvobok RV, et al. Development of compositions of slag-alkaline binding materials for pavement products. *Voprosy Khimii i Khimicheskoi Tekhnologii*. 2023; (5): 147-154. doi: 10.32434/0321-4095-2023-150-5-147-154.

6. Shabanova GM, Korogodska AM, Shumeiko VM, Shchukina LP, Lisachuk GV, Kryvobok RV, et al. The effect of hardening activators on the physical and mechanical properties of slag-alkaline binding materials. *Voprosy Khimii i Khimicheskoi Tekhnologii*. 2023; (5): 155-162. doi: 10.32434/0321-4095-2023-150-5-155-162.